J Mater Sci: Mater Electron (2016) 27:8493–8498
DOI 10.1007/s10854-016-4864-z

Influence of lanthanum doping via hydrothermal and reflux methods on the SnO_2–TiO_2 nanoparticles prepared by sol–gel method and their catalytic properties

Komal Mehmood Butt[1] · Muhammad Akhyar Farrukh[1] · Iqra Muneer[1]

Received: 27 March 2016 / Accepted: 18 April 2016 / Published online: 23 April 2016

Abstract In the present work, tin oxide–titanium oxide (SnO_2TiO_2) nanoparticles were synthesized via sol–gel method and doping of lanthanum (La) on tin oxide–titanium oxide (La/SnO_2TiO_2) nanoparticles was carried out using hydrothermal and reflux methods. Effect of different preparation methods on the size and catalytic properties of nanoparticles was investigated. The La/SnO_2TiO_2 nanoparticles were characterized by Fourier transform infrared spectroscopy, scanning electron microscopy, powder X-ray diffraction and solid phase spectroscopy. The UV–Vis spectroscopy was used to investigate its catalytic properties for methylene blue degradation. It was found that La/SnO_2–TiO_2 nanoparticles prepared by hydrothermal method have small size and maximum degradation capacity. The red shift in La nanoparticles was observed with band gap of 4.25 eV as compared to bulk material.

1 Introduction

Syntheses of metal oxides, with size of nanometers, have received wide acceptance and applications in photocatalysts [1], gas sensors [2], destructive adsorbents [3] and solar energy converters [4]. The optical and electrical properties of nanoparticles largely depend upon the size [4], therefore a number of preparation methods with both gas phase and liquid phase [5] have been adopted to better control size, distribution and shape of the particles. Sol gel method has been adopted for synthesis of base material, because this method was found more suitable for high value of degradation rate of organic pollutants (k min^{-1}) and less concentration of rutile TiO_2 than other common methods like hydrothermal and ultrasonication [6]. $SnCl_4.5H_2O$ and benzyl alcohol were used in 1:5 because prior work has shown that particle size was observed smallest by using this ratio [7].

Doping of rare earth metal is done in order to decrease the particles size and increase the surface area. A decrease in band gap (red shift) in composite material having rare earth (RE) metal as compared to base (SnO_2–TiO_2) material is observed. However, RE^{+3} does not affect band gap. Rare earth metals being larger in size than both titanium and tin, distributes itself over the surface of particles and prohibited the aggregation of titanium which results an increase in surface area [8]. 4f orbital of lanthanum is found very effective for the bonding with functional groups such as amines, aldehydes and thiols (lewis bases) [9].

Organic dyes in water are considered as pollutants because of their potential to decompose aerobically or anaerobically into some carcinogenic compounds [10]. Conventional methods to reduce them are not single step but metal oxide nanoparticles especially containing TiO_2 are found effective for this purpose.

In this work, lanthanum doped tin oxide–titanium oxide (La/SnO2–TiO2) nanaoprticles have been synthesized using reflux and hydrothermal method. A comparison has been carried out between base material (SnO_2–TiO_2) and La/SnO_2TiO_2 with reference to size, band gap, percentage degradation of methylene blue dye and degradation rate.

✉ Muhammad Akhyar Farrukh
akhyar100@gmail.com

[1] Nano-Chemistry Laboratory, Department of Chemistry, GC University Lahore, Lahore 54000, Pakistan

2 Experimental

2.1 Synthesis of tin oxide (SnO_2) nanoparticles by sol–gel method

6 mL aq. solution of tin tetra chloride penta-hydrate ($SnCl_4$·$5H_2O$) (30 mM, pH = 1–2) and 4 mL aq. solution of benzyl alcohol (150 mM) were mixed (*sol*). NaOH solution (120 mM) was added at rate of 0.2 mL per 5 min with continuous stirring, till pH 5 was obtained (*gel*). Centrifugation of gelatinous solution was done at 6000 rpm for 3 min. Precipitates were dried at 70 °C and calcined at 600 °C for 90 min.

2.2 Synthesis of tin oxide–titanium oxide (SnO_2–TiO_2) nanoparticles

4.5 mL titanium isopropoxide and 13.5 mL 2-propanol were mixed. HNO_3 was added at rate of 0.5 mL per 5 min with constant stirring at 70 °C until a white milky solution was obtained. 21.5 mg calcined SnO_2 nanoparticles were mixed in 10 mL distilled water and stirred at room temperature for 30 min. To this solution white solution of TiO_2 nanoparticles was added at rate of 2 mL per 5 min, with continuous stirring. Solution was centrifuged at 8000 rpm for 5 min. Precipitates were dried at 100 °C and calcined at 400 °C for 90 min. White powder of SnO_2–TiO_2 nanoparticles was obtained.

2.3 Preparation of La/SnO_2–TiO_2 nanoparticles through hydrothermal method

Solution of 0.004 M of lanthanum chloride heptahydrate ($LaCl_3$·$7H_2O$) was prepared and 10 mg of SnO_2–TiO_2 nanopartciles were added in it. The pH of solution was maintained at 3–4 by using 0.2 M HNO_3 solution and stirred for 30 min at room temperature. Hydrothermal autoclave containing above solution was placed in oven for 120 min at 160 °C. Centrifugation was done at 13,000 rpm for 5 min and precipitates were dried and calcined at 70 and 550 °C respectively.

2.4 Preparation of La/SnO_2–TiO_2 nanoparticles through reflux method

The same procedure as mentioned in hydrothermal method was adopted. However, the solution was shifted in round bottom flask and refluxed for 90 min at 150–160 °C.

2.5 Characterization

Structural analysis of La/SnO_2–TiO_2 was performed using Fourier transform infra-red (FTIR) V MIDAC 2000 with KBr powder with 1:7 (nanoparticles: KBr). The morphology of nanoparticles was investigated by FEI quanta 200 F field emission scanning electron microscope (FESEM) and Philips CM12, 80 kV transmission electron micrroscope (TEM). The structural properties of La/SnO_2–TiO_2 were investigated using X-ray diffractometer (Xpert Pro Panalytical). The spectrum was recorded in the 2θ range of 20° to 80° with 4°/min scan speed). Optical measurements were carried out using UV–visible double beam spectrophotometer (Hitachi U-2800).

3 Results and discussion

3.1 FTIR analysis

In Fig. 1, FTIR spectra of calcined SnO_2–TiO_2 and La/SnO_2–TiO_2 nanoparticles (prepared by reflux and hydrothermal method) are shown. Peaks around 3370 and 1665 cm^{-1} are due to stretching vibration of OH bond in water due to absorption on surface [11, 12]. Peaks at 2300 cm^{-1} are due to stretching vibrations of C–H bond [11] and their intensity also reduced after calcination, confirming the removal of organic solvent. Peaks around 1665 cm^{-1} may be due to vibrations of O–Sn–O bridging [13]. Peak at 660 cm^{-1} is for Sn–O [14, 15], 680 cm^{-1} is for Ti–O [16] and at 573 cm^{-1} peak is for La–O [17].

3.2 FESEM-EDX analysis

Doped and undoped nanoparticles were also analyzed through SEM-EDX. It is visible that undoped particles are agglomerated (Fig. 2 a) while porosity increases in doped material (Fig. 3a) and it can be attributed to La which has distributed over the surface and inhibited the agglomeration. Theoretically the undoped material contains 51.3 % Sn, 20.8 % Ti and 27.8 % O and doped material contains

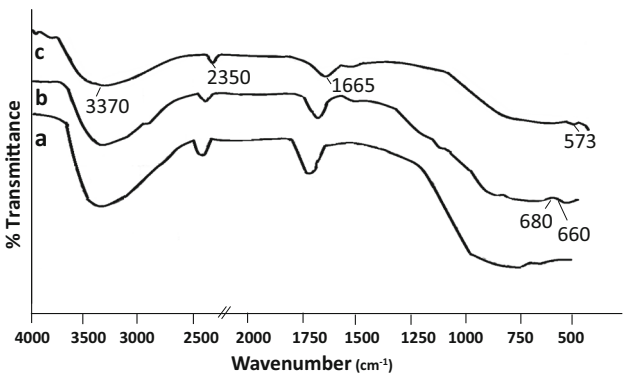

Fig. 1 FTIR spectrum of **a** SnO_2–TiO_2 prepared in the presence of benzyl alcohol **b** La/SnO_2–TiO_2 prepared by reflux method and **c** La/SnO_2–TiO_2 prepared by hydrothermal method

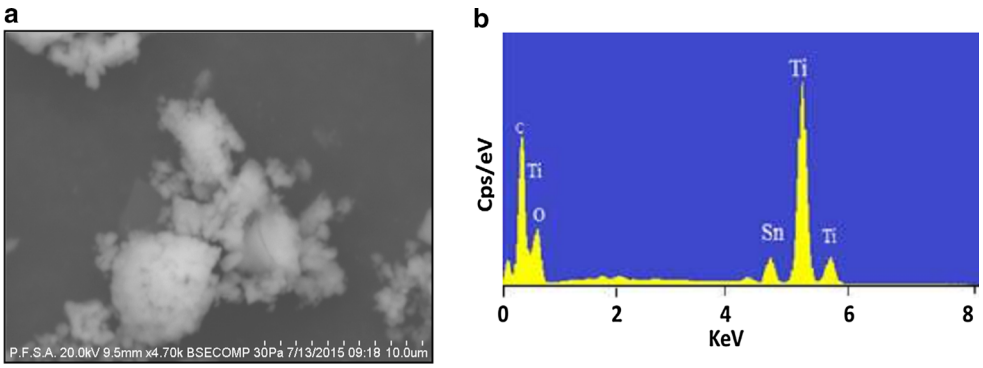

Fig. 2 **a** SEM image of SnO_2–TiO_2 prepared in the presence of benzyl alcohol **b** EDX

31.9 % Sn, 12.72 % Ti, 17.32 % O, and 37.35 % La. EDX analysis showed that 46.50 % Sn,25.26 % Ti, and 32.67 % O was present in undoped material and doped material consisted of 31.9 % Sn,14.5 % Ti, 15.19 % O, and 37.35 % La. So doping increased the surface area and has positive effect on rate constant of catalysis [8].

3.3 Transmission electron microscopy

TEM images of La/SnO_2 TiO_2 are given in the Fig. 4. Average size of particles calculated for base SnO_2–TiO_2, La/SnO_2–TiO_2 prepared by reflux method and La/SnO_2–TiO_2 prepared by hydrothermal method are 18, 12.24 and 10.28 nm respectively which are closely related to XRD results.

3.4 XRD analysis

XRD analysis was done using Cu K_α radiation for phase estimation and crystallite size determination of prepared nanoparticles of SnO_2–TiO_2 and La doped SnO_2–TiO_2 prepared through reflux and hydrothermal methods as given in Fig. 5. Scanning range of radiations was selected 20°–80°. Crystallite size (d) was determined through Scherrer's equation and Williamson–Hall method and it was deduced that crystallite size decreased after doping. This reduction in size can be attributed to formation of La–O–Ti bond on surface of particles that reduced the chances of crystal growth [18]. Using shape factor k (0.98), wavelength λ (1.54 Å), angle θ and Full Width at Half Maximum (FWHM, β) in Scherrer's equation, crystallite size (d) was calculated as follow:

$$d = \frac{k\lambda}{\beta \cos\theta} \tag{1}$$

$$\beta = \frac{k\lambda}{d \cos\theta} \tag{2}$$

Strain induced due to crystal distortion is calculated by following equation.

$$\varepsilon = \frac{\beta}{4 \tan\theta} \tag{3}$$

$$\beta = \varepsilon\, 4 \tan\theta \tag{4}$$

Equation 1 (Scherrer equation) has 1/cosθ dependency while Eq. 2 (Williamson Hall) has 1/tanθ dependency, so assuming that strain ε and crystallite size d have independent effect on line broadening β, we add Eqs. 2 and 4 as follow [19]:

$$\beta = \frac{k\lambda}{d \cos\theta} + \varepsilon 4 \tan\theta \tag{5}$$

Multiplying with cos θ

$$\beta \cos\theta = \frac{k\lambda}{d} + \varepsilon\, 4 \sin\theta \tag{6}$$

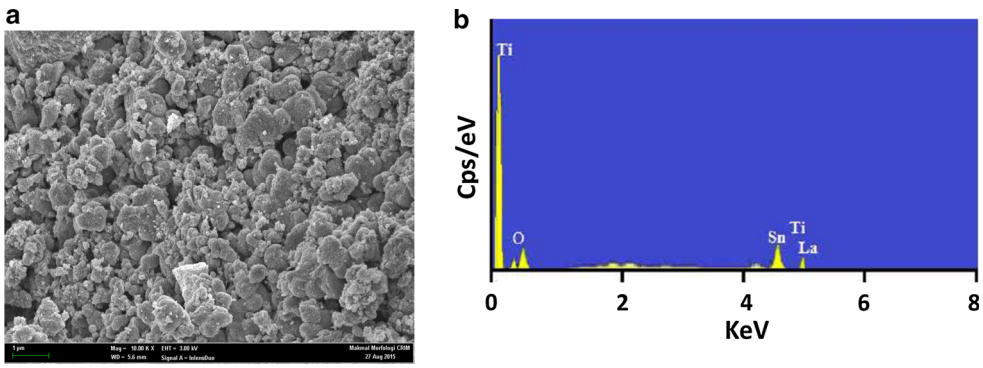

Fig. 3 **a** SEM image of La/SnO_2–TiO_2, prepared by hydrothermal method **b** EDX

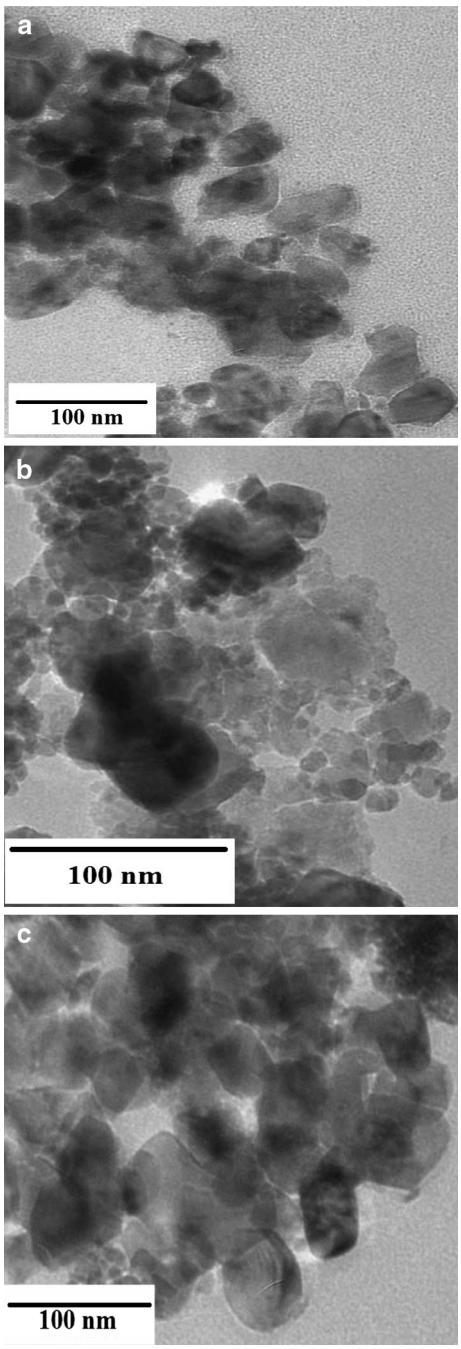

Fig. 4 TEM images of nanoparticles **a** SnO_2–TiO_2 **b** La/SnO_2–TiO_2 prepared by reflux method **c** La/SnO_2–TiO_2 prepared by hydrothermal method

This straight line equation (Eq. 6) is known as Williamson–Hall equation and used for crystallite size determination by plotting graph between $\beta \cos\theta$ and 4 sinθ. kλ/d is intercept and d is crystallite size. So value of intercept from graph was used for determination of crystallite size d. ε is the strain and can be determined from slope of line [19].

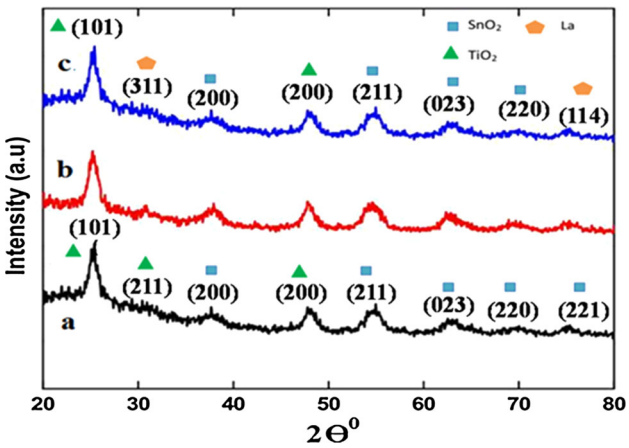

Fig. 5 XRD pattern of *a* SnO_2–TiO_2 prepared in the presence of benzyl alcohol *b* La/SnO_2–TiO_2 prepared by hydrothermal method, calcined at 550 °C and *c* La/SnO_2–TiO_2 prepared by reflux method, calcined at 550 °C

In XRD spectrum of SnO_2TiO_2, peak at 25.33° and 48.2° with *hkl* (101) and (200) were of anatase phase of TiO_2 [20], while peaks at 30.77° (211) was of brookite phase [21]. Peaks at 37.84°, 54.5°, 62.9°, 70.13°and 75.33° were of SnO_2 with *hkl* values (200), (211), (023), (220) and (221) respectively [22]. Particle size calculated through Scherrer's equation was 12 nm and it was 15 nm through Williamson Hall method.

In La/SnO_2TiO_2 prepared through reflux and hydrothermal method, Peaks at 30.8° and 75.3° were of Lanthanum (La) with *hkl* values of (311) and (114) respectively. [24]. Crystallite size of nanoparticles prepared by reflux method, calculated through Scherrer's equation was found 8.30 nm and it was 11.43 nm through Williamson Hall equation while nanoparticles by hydrothermal method, size was found 4.7 nm (Scherrer) and 8.2 nm through Williamson Hall method, as given in Table 1. Both methods confirmed that doping of lanthanum on SnO_2–TiO_2 prepared by reflux method reduced the particle size. Moreover doping also inhibited the conversion of anatase phase of TiO_2 to rutile or brookite phase. Doping through hydrothermal method caused even more reduction in size than prepared by reflux method (Fig. 6).

3.5 Band gap calculation

Figure 7 shows the spectral dependence of La/SnO_2–TiO_2 synthesized by hydrothermal method. Band gap of hydrothermally doped SnO_2–TiO_2 was also calculated using Wood and Tauc equation as follow:

$$\alpha h\nu = B(h\nu - E_g)^{1/n} \quad (7)$$

here α is absorption coefficient, $h\nu$ is energy of photon being bombarded, E_g energy gap between valence band and

Table 1 Relationship between crystallite size and percentage degradation of methylene blue dye

Sample	Crystallite size (nm)			k (min^{-1})	Degradation (%)
	Scherrer	Williamson–Hall	TEM		
SnO_2–TiO_2 (base)	12.00	15.00	18.0	0.039	30.8
La/SnO_2–TiO_2 (reflux)	8.30	11.43	12.24	0.047	36.2
La/SnO_2–TiO_2 (hydrothermal)	4.70	8.20	10.28	0.070	58.29

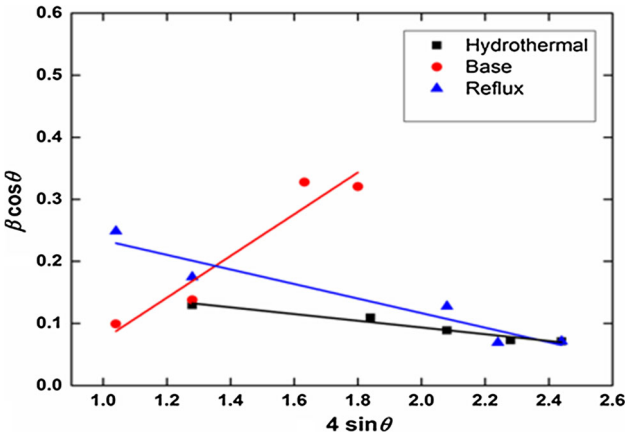

Fig. 6 Williamson–Hall plots of SnO_2–TiO_2 (base) prepared by sol–gel method and La/SnO_2–TiO_2 prepared by reflux and hydrothermal methods

conduction band, n is transition state and it can be a whole number or in fraction depending upon type energy level in which electron are being transferred after excitation. B is constant of proportionality known as absorption constant and it depends upon transition [20, 25]. Graph was plotted taking *hv* on x-axis and $(\alpha hv)^2$ on y-axis and band gap was determined by extrapolation of curved line. Band gap hydrothermally doped material was observed 4.25 eV.

4 Catalytic activity of SnO_2–TiO_2 and La/SnO_2–TiO_2 nanoaprticles

Catalytic activity of SnO_2–TiO_2 and La/SnO_2–TiO_2 nanoaprticles was examined by studying the degradation of methylene blue dye at ambient temperature. 20 ppm solution of methylene blue dye was prepared and 15 mg SnO_2–TiO_2 nanoparticles were added in it. Stirring of solution was done for 60 min in the presence of sunlight and absorbance was measured after interval of 2 min at 665 nm using UV–Vis spectrophotometer, till constant value was obtained. Similar process was repeated for La/SnO_2–TiO_2. Graphs were plotted between ln ($A–A_\infty$) and time (min) as given in Fig. 8. Slope of line gave the value of rate (k, min^{-1}) and confirmed that degradation follows pseudo first order equation [4]. k value is found smallest for SnO_2–TiO_2 and highest for La/SnO_2–TiO_2 prepared by hydrothermally method so we can deduce that with

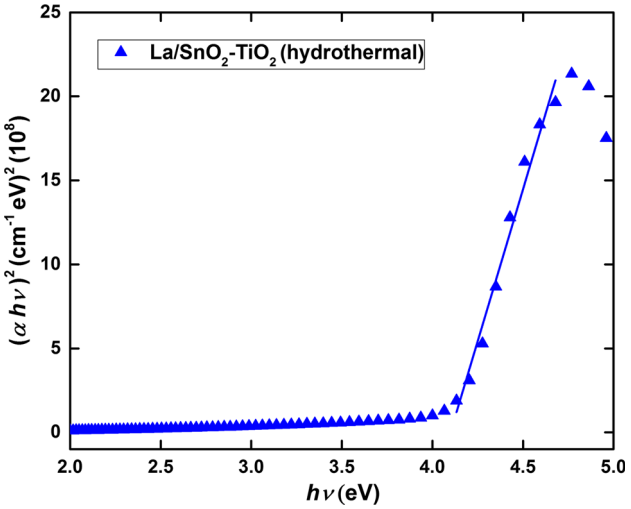

Fig. 7 Band gap energy of La/SnO_2–TiO_2 nanoparticles

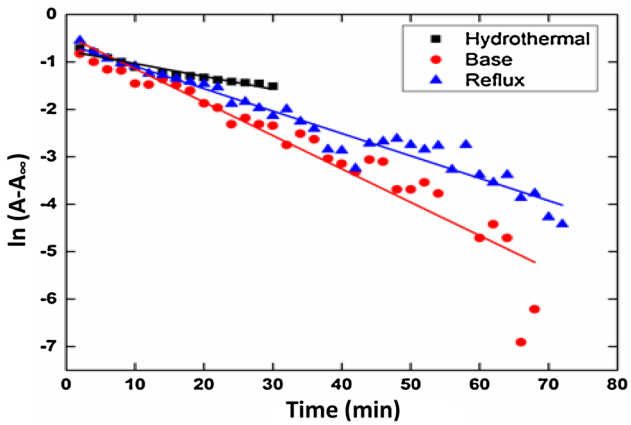

Fig. 8 Plots of ln ($A–A_\infty$) versus time (min) for determination of rate constant values of SnO_2–TiO_2 (base) prepared by sol–gel method and La/SnO_2–TiO_2 prepared by reflux and hydrothermal methods

decrease in size, degradation rate increases. Percentage degradation of dye was also calculated and it was also found highest for nanoparticles prepared by hydrothermal method (Table 1).

5 Conclusion

Nanoparticles of SnO_2–TiO_2 were prepared by sol–gel method using benzyl alcohol as solvent while doping was carried out by reflux and hydrothermal methods. Catalytic activities of all prepared nanoparticles were determined through degradation of methylene blue dye. Relationship between crystallite size, band gap, percentage degradation and catalysis rate was determined using different techniques and methods and it was inferred that by decrease in crystallite size reduces the band gap while degradation rate and percentage degradation increases. Particle size of La/SnO_2–TiO_2 is found minimum at 4.7 nm while synthesized by hydrothermal method as compared to the particles synthesized by reflux method 8.3 nm. Thus, La/SnO_2–TiO_2 prepared by hydrothermal method acts as good photocatalyst due to small size and large surface area. By doping of lanthanum, band gap of La/SnO_2–TiO_2 reduce to 4.25 from 6.4 eV (band gap of lanthanum in bulk). Comparing doping methods, hydrothermal method was found best method than reflux method.

Acknowledgments The authors are thankful to Higher Education Commission (HEC) Pakistan to support through research grant No. 20-2660/NRPU/R&D/HEC/13.

References

1. M.M. Oliveira, D.C. Schnitzler, A.J.G. Zarbin, Chem. Mater. **15**, 1903–1909 (2003)
2. G.F. Fine, L.M. Cavanagh, A. Afonja, R. Binions, Sensors **10**, 5469–5502 (2010)
3. A. Imtiaz, M.A. Farrukh, M. Khaleeq-ur-Rehman, R. Adnan, Sci. World J. **2013**, 641420 (2013)
4. G. Oskam, A. Nellore, R.L. Penn, P.C. Searson, J. Phys. Chem. B **107**, 1734–1738 (2003)
5. J.H. Bang, K.S. Suslick, Adv. Mater. **22**, 1039–1059 (2010)
6. S. Javaid, M.A. Farrukh, I. Muneer, Superlattice Microsttuct. **82**, 234–247 (2015)
7. I. Muneer, M.A. Farrukh, S. Shagraf, M. Khaleeq-ur-Rahman, Mater. Sci. Forum **756**, 197–204 (2013)
8. H. Wei, Y. Wu, N. Lun, J. Mater. Sci. **39**, 1305–1308 (2004)
9. H. Liu, L. Yu, W. Chen, J. Nanomater. (2012). doi:10.1155/2012/235879
10. I. Ullah, S. Ali, M.A. Hanif, S.A. Shahid, Int. J. Chem. Biochem. Sci. **2**, 60–77 (2012)
11. H. Parveen, M.A. Farrukh, M. Khaleeq-ur-Rahman, Russ. J. Phys. Chem. A **89**, 99–107 (2015)
12. T. Krishnakumar, R. Jayaprakash, V.N. Singh, B.R. Mehta, A.R. Phani, J. Nano R. **4**, 91–101 (2008)
13. B. Munir, M.A. Farrukh, H. Parveen, Russ. J. Phys. Chem. A **89**, 1051–1058 (2015)
14. M.A. Farrukh, B. Heng, R. Adnan, Turk. J. Chem. **34**, 537–550 (2010)
15. R. Adnan, N.A. Razana, I.A. Rahman, M.A. Farrukh, J. Chin. Chem. Soc. **57**, 222–229 (2010)
16. A.A. Belhekar, S.V. Awate, R. Anand, Catal. Commun. **3**, 453–458 (2002)
17. M.A. Farrukh, F. Imran, S. Ali, M. Khaleq-ur-Rahman, Russ. J. Appl. Chem. **88**, 1523–1527 (2015)
18. V. Stengl, S. Bakardjieva, N. Murafa, Mater. Chem. Phys. **114**, 217–226 (2009)
19. Y.T. Prabhu, K.V. Rao, V.S.S. Kumar, B.S. Kumari, World J. Nano. Sci. Eng. **4**, 21–28 (2014)
20. M.A. Farrukh, M. Shahid, I. Muneer, S. Javaid, M . Khaleeq-ur-Rahman, J. Mater. Sci.: Mater. Electron. **27**, 2994–3002 (2016)
21. A.D. Paola, M. Bellardita, L. Palmisano, Catalysts **3**, 36–73 (2013)
22. A.K. Singh, U.T. Nakate, ANP. **2**, 66–70 (2013)
23. Y. Feng, Y. Cui, B. Logan, Z. Liu, Chemosphere **70**, 1629–1636 (2008)
24. F.H. Spedding, J.J. Hanak, A.H. Daane, J. Less Common Met. **3**, 110–124 (1961)
25. I. Muneer, M.A. Farrukh, S. Javaid, M. Shahid, Superlattice Microstruct. **77**, 256–266 (2015)